Journal of Applied Mechanics Vol.12, pp.945-956 （August 2009） JSCE

Concrete Stress-Strain Relationship of Circular Columns Confined with FRP Composites

FRP 連続繊維補強による RC 円形柱の応力-ひずみ関係

Mohamed F.M. FAHMY* and Zhishen WU**
フアハミ モハメド· 呉 智深

* Ph.D. Candidate Dept. of Urban & Civil Eng. Ibaraki University (4- 12- 1, Nakanarusawa, Hitachi, 316- 8511)
** Member Dr. of Eng. Prof. Dept. of Urban & Civil Eng. Ibaraki University (4- 12- 1, Nakanarusawa, Hitachi, 316- 8511)

Two analytical popular models are employed to find concrete stress-strain relationship of three scale-model circular columns confined with different types of fiber-reinforced polymer (FRP) composites. The second ascending part of the stress-strain relationship of well confined concrete is evaluated in the light of available database from the existing literature using these models. The results showed that the examined models do not satisfy the criterion that the slope of the second branch of the stress-strain curve of sufficiently confined concrete is independent of FRP types, provided the design confinement modulus is the same. A comparison of predicted values of the second stiffness with the collected test results of 249 cylinder specimens confined with composites revealed the necessity for a more accurate model. A model considering the effect of FRP confinement modulus is proposed.

Key Words: *Circular columns, Confined concrete, Confinement stiffness, FRPs.*

1. Introduction

The commonly used FRP includes Carbon fiber (CFRP), Glass fiber (GFRP), and Aramid fiber (AFRP), while some new FRPs with special properties like energy absorption and large fracturing strain have been gradually applied in recent years such as PBO, Dyneema fiber (DFRP), PET, PEN, and PAF, which are listed in **Table 1**, (JSCE 2005) [1]. PBO fiber has been explored to have similar advantages with high strength CFRP, and has a greater impact-tolerance and energy absorption ability. In addition, PBO fiber demonstrates high creep resistance and fire/fuel resistance (Wu et al. 2003b and 2007b) [2&3]. DFRP would have wide applications in strengthening structures due to its special energy absorption ability and water resistance, aside from high strength and high ductility, which is suitable for underwater structures strengthening (Wu et al. 2006c) [4]. Although the others, like PET, PEN and PAF, do not have similar high tensile strength relative to carbon fiber, they do have considerable high fracturing strain that seldom exists in other FRPs. This specialty is the most important for strengthening or retrofitting seismic behaviors of columns or piers, where the ductility is of utmost concern (Anggawidjaja et al. 2006) [5].

Continuous basalt fiber (CBF) is a kind of high-tech fibers developed in the former Soviet Union about 30 years ago, using lava as raw materials. Basalt fiber reinforced polymer (BFRP) has a lot of advantages comparable to CFRP, AFRP, and other FRPs, such as excellent mechanical properties, high temperature compatibility and large working temperature scope between -269 to 700° C, acid alkali-resistant, low hygroscopity, and better environment adaptability (Wu et al. 2007a) [6].

Table 1. Mechanical properties of FRP sheets, (JSCE 2005) [1]

Type of sheet	f_{ju} (N/mm^2)	E_j (kN/mm^2)	ε_{ju} (%)
High strength Carbon	3400	230	1.5
High modulus Carbon	1900	540	0.35
Aramid	2000-2500	73-120	1.8-3.0
E-Glass	1500	80	1.9
PBO	3500	240	1.5
Dyneema	1832	60	3.08
PET	923	6.7	13.8
PEN	1028	22.6	4.5
PAF	1730	40	6
Basalt*	1835	92	1.99

Note: PBO (Polypara-phenylene-Benzo-bis-Oxazole), PET (Polyethylene Terephthalate / Polyester), PEN (Polyethylene Naphthalate), PAF (Polyacetal Fiber).
* Basalt mechanical properties are given by (Wu et al. 2007a) [6].

The diversity of FRP types allows for the design engineers the choice among these materials. One of the main factors that may govern the choice of any of these materials is the structure final strengthening cost. Despite the low stiffness value of PET, PEN, and PAF, which has an adverse impact on the quantity of the used fiber; the final strengthening cost might be less (Anggawidjaja et al. 2006) [5]. Also, it is reported by Wu et al. (2007a) [6] that retrofitted columns with BFRP can have the same or even better performance than columns retrofitted with CFRP. Additionally, the continuous basalt fiber can have a good prospect in seismic strengthening of RC columns due to the low price of basalt fiber.

Over the past 20 years, numerous design-oriented models were derived from available experimental data of FRP-confined concrete to predict the ultimate stress and strain or the entire stress-strain response (Fardis and Khalili 1982 [7], Kharbhari and Gao 1997 [8], Samaan et al. 1998 [9], Saafi et al. 1999 [10], Hosotani and Kawashima 1999 [11], Toutanji 1999 [12], Xiao and Wu 2000 [13], Lam and Teng 2003 [14], Wu et al. 2003a [15], Wu et al. 2006a [16], and Harajli 2006 [17]). At the moment, the pressing question is "are the available models capable of identifying the stress-strain behavior of confined concrete with these new FRP materials?" Therefore in this study, two key measures are utilized to examine the practicality of using one of the existing models as a general model. First, a criterion that the slope of the second branch of the stress-strain curves of FRP-confined concrete is independent of the types of FRP, provided the design confinement modulus is the same. Second, the accuracy of the existing models in predicting this slope.

For circular columns retrofitted with FRP, pseudo dynamic test results revealed that a ductile member may be suddenly destroyed by a significant pulse-like wave before it is able to utilize its ductile behavior to dissipate seismic energy (Chang et al. 2004) [18]. Accordingly, improving the inelastic stage ductility is not the only requirement under the seismic action, but enhancement of the strength is also necessary. Hence, this study is focused on sufficiently or well confined concrete (concrete with strain hardening performance). To predict whether FRP-confined concrete cylinder has a strain softening or a strain-hardening response, Wu et al. (2006a) [16] suggested boundary values, which reflect the effect of FRP modulus, based on an investigation on experimental results.

This study is conducted in the following steps: (1) two popular models of existing design oriented models are reviewed; (2) for different FRP types (CFRP, BFRB, DFRP, and PET) providing equivalent lateral modulus, these models are employed to obtain the stress-strain relationship of scale-model circular columns with different concrete strengths (20, 35, and 50 MPa); (3) the second stiffness is evaluated in the light of available database of test results collected from literature; (4) discussion of features and accuracy of these models is given. A new model that overcomes the drawbacks of the reviewed models is presented. Finally, a comparison of one of the investigated models and the proposed model with the available test data is presented.

2. Analytical Models Predicting Stress-Strain of FRP-Confined Circular Columns

Numerous models are available to determine the FRP-confined concrete behavior under concentric load. Most of the proposed stress-strain relationships are based on early studies by Richart et al. (1928) [19] on the strength and longitudinal strain at failure for concrete confined by an active hydrostatic fluid pressure. The current study focuses on two popular models (Samaan et al. 1998 [9] and Lam and Teng 2003 [14]), and a wider comparison between the performance of some of the existing models would be treated in a future study by the authors.

For a circular concrete column of diameter d, confined by a circumferential FRP wrap with elastic modulus E_j, and assuming deformation compatibility between the confining wrap and the concrete surface, the exerted confining pressure f_l at a circumferential strain ε_j can be obtained using the following form (De Lorenzis and Tepfers 2003) [20]:

$$f_l = E_l.\varepsilon_j \tag{1}$$

$$E_l = \frac{2E_j.n.t}{d} \tag{2}$$

where t is the thickness of one layer, n is the number of FRP layers, and E_l is called confinement modulus or lateral modulus. The maximum exerted confining pressure f_{lu} is attained when the circumferential strain in the FRP reaches its ultimate ε_{ju} corresponding to a tensile strength f_{ju}.

$$f_{lu} = \frac{2f_{ju}.n.t}{d} \tag{3}$$

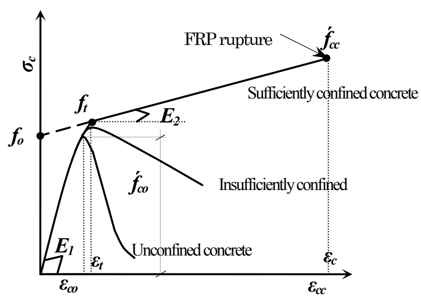

Fig.1 Typical stress-strain responses for unconfined and FRP-confined concrete

2.1 Samaan et al. Model (1998) [9]

For fiber-wrapped and FRP-encased concrete columns, Samaan et al. (1998) [9] assumed that the stress-strain curve is bilinear. The second slope of the curve, E_2, intersects the stress axis at f_o, and is a function of the stiffness of the confining fiber, and to a lesser extent, the unconfined strength of concrete core. It is expressed as follows:

$$E_2 = 245.61 f_{co}'^{\,0.2} + 0.6728\left(\frac{2.E_j.n.t}{d}\right) \tag{4}$$

where f'_{co} and ε_{co} = unconfined concrete compressive strength and failure strain, respectively, **Fig. 1**.

Eq. (5) was used for strength calculation (f'_{cc}),

$$f'_{cc} = f'_{co} + k_1 . f_{lu} \tag{5}$$

where k_1 was assumed in relation to the ultimate confining pressure by the following relationship:

$$k_1 = 6 f_{lu}^{-0.3} \tag{6}$$

The ultimate strain is determined from the geometry of the bilinear curve as

$$\varepsilon_{cc} = \frac{f'_{cc} - f_o}{E_2} \tag{7}$$

where f'_{cc} is the ultimate strength of confined concrete, ε_{cc} is the corresponding failure strain under a maximum lateral pressure f_{lu}, **Fig.1**, and the stress f_o is a function of the strength of unconfined concrete and ultimate confining pressure provided by the FRP and was estimated as

$$f_o = 0.872 f'_{co} + 0.371 f_{lu} + 6.258 \tag{8}$$

To evaluate the first slope (E_1), the following formula was adopted:

$$E_1 = 3{,}950 \sqrt{f'_{co}} \, [\mathrm{MPa}] \tag{9}$$

2.2 Lam and Teng Model (2003) [14]

The model is composed of two parts. The first is parabolic and the second is linear with a slope E_2 that intersects the stress axis at f'_{co}. The model was expressed in the following general form

$$\sigma_c = E_c \varepsilon_c - \frac{(E_c - E_2)^2}{4 f'_{co}} \varepsilon_c^2 \quad \text{for } 0 \le \varepsilon_c \le \varepsilon_t \tag{10}$$

and

$$\sigma_c = f'_{co} + E_2 \varepsilon_c \qquad \text{for } \varepsilon_t \le \varepsilon_c \le \varepsilon_{cc} \tag{11}$$

where σ_c and ε_c are the axial stress and strain, respectively.

The first parabolic portion meets the second linear portion with a smooth transition at ε_t, which is given by

$$\varepsilon_t = \frac{2 f'_{co}}{(E_c - E_2)} \tag{12}$$

$$E_2 = \frac{f'_{cc} - f'_{co}}{\varepsilon_{cc}} \tag{13}$$

where E_c is the elastic modulus of unconfined concrete and was taken as $4{,}730\sqrt{f'_{co}}$ [MPa].

Due to the effect of nonuniform stress distribution and curvature in the FRP jacket, the rupture strain of the FRP confinement is lower than the ultimate tensile strain determined from direct coupon tests. Lam and Teng (2003) [14], based on an evaluation of experimental data, suggested using a value of $\varepsilon_{j,rup}$ for CFRP, GFRP, and AFRP equals, respectively, to 0.586, 0.624, and 0.851 of the ultimate tensile strain of the FRP material. These values are defined as FRP efficiency factors. A redefinition for the ultimate confinement pressure was given based on the actual rupture strain of FRP, and it is called the actual maximum confining pressure $f_{lu,a}$ given by

$$f_{lu,a} = \frac{2 E_j n t \varepsilon_{j,rup}}{d} \tag{14}$$

Lam and Teng (2003) [14] used a database of cylinder concrete confined with the CFRP, GFRP, and AFRP to plot a relation between the strengthening ratio f'_{cc} / f'_{co} and the actual confinement ratio $f_{lu,a} / f'_{co}$. The trend line of these test data was approximated using the following equation

$$\frac{f'_{cc}}{f'_{co}} = 1 + 3.3 \frac{f_{lu,a}}{f'_{co}} \tag{15}$$

Lam and Teng model considers the impact of the confinement stiffness on the ultimate strain, thus, the following expression was suggested for FRP-wrapped concrete

$$\frac{\varepsilon_{cc}}{\varepsilon_{co}} = 1.75 + 12 \left(\frac{2 E_j n t}{E_{\sec o} d} \right) \left(\frac{\varepsilon_{j,rup}}{\varepsilon_{co}} \right)^{1.45} \tag{16}$$

$$E_{\sec o} = \frac{f'_{co}}{\varepsilon_{co}} \tag{17}$$

where E_{seco} is the secant modulus of elasticity at the compressive strength of unconfined concrete.

3. Evaluation of Different Models

This study attempts to find a model properly representing the behavior of FRP confined concrete with any type of FRP composites. To achieve this objective, two measures for the above mentioned models will be discussed in the following section.

3.1 Stress-Strain Response of Confined Concrete Using Different FRP Types Providing the Same Lateral Stiffness

After strengthening an existing deficient column using FRP, its behavior is a function of the used fiber and its amount, i.e., the required structural performance levels of an existing structure could be controlled based on both the selected FRP type and the defined design level of lateral modulus. With the available range of FRP types, the choice among these materials would be decided based on the required performance level of the strengthened structure and the final strengthening cost. Hence, it becomes very important to have a reliable model to compare the available FRPs in order to choose the one that would achieve both the required level of performance and the least cost.

The addressed models were built based on experimental results of cylinder specimens confined with the common FRP types. And since there is a shortage of experimentally tested specimens using the new types of FRP under uniaxial load, a fundamental criterion is employed to examine the possibility of using one of the existing models as a universal model to predict the response of FRP-confined concrete. The criterion is that the slope of the second ascending branch of stress-strain curve of FRP-confined concrete is independent of the FRP types, provided they are designed with identical confinement modulus. It follows that, lateral pressures of these fibers are responsible for the definition of the end point of the stress-strain response.

To this end, the authors utilized these models to predict the FRP-confined concrete stress-strain curves using CFRP, BFRP, DFRP, and PET as confinement materials for three scale model circular reinforced concrete columns with the detailed properties given in **Table 2**. The mechanical properties of the suggested FRP materials are given in **Table 3**. To choose among these materials the above criterion is employed. The selected design level of confinement stiffness is 1042 MPa, which is decided based on experimentally tested circular columns that were retrofitted with CFRP for the shear deficiency and tested under the effect of reversed cyclic lateral load and constant axial load (Wu et al 2006b) [21].

These columns have the same physical characteristics but with different concrete strengths, and because of their original deficiency it is required to increase both the strength and strain of concrete core through FRP wrapping. Using Samaan et al. (1998) [9] and Lam and Teng (2003) [14], the axial stress strain relationships of FRP confined concrete for each column were predicted for the offered FRPs. **Fig. 2** shows the predicted confined concrete stress strain curves of these columns. It should be noted in the designation of these specimens that letters "C", "B", "D", and "P" signify CFRP, BFRP, DFRP, and PET respectively; and the numbers "20, 35, and 50" denote the concrete strengths. It is obvious from **Fig.2** that the predicted axial stress-strain curves of any of concrete strengths depend on the FRP type; even though the design levels of the lateral stiffness are similar. This means that both models are sharing one deficiency that many curves could be for FRP-confined concrete based on the mechanical properties of the fiber, even if all FRP types are designed to the same level of the lateral stiffness.

Table2 Details and dimensions of three scale-model composite-jacketed circular columns

Column	d (mm)	f'_{co} (MPa)	A_s (mm^2)	Stirrups	Steel mechanical properties	
					f_y (MPa)	E_s (GPa)
1	360	20	5.8% A_c	Ø6.5/150 mm	382	200
2	360	35	5.8% A_c	Ø6.5/150 mm	382	200
3	360	50	5.8% A_c	Ø6.5/150 mm	382	200

A_c is column cross-section area, A_s is area of column longitudinal reinforcement, and E_s and f_y are modulus of elasticity and yield strength of steel reinforcement.

Table 3 Mechanical properties of FRP composites

Mechanical Properties	CFRP*	BFRP*[a]	DFRP**	PET*[a]
Elastic modulus E_f (GPa)	249.6	92.0	60.3	6.7
Fracture Strength f_{fu} (MPa)	3945.0	1835.0	1438.7	923.0
Fracture strain ε_{fu} (%)	1.52	1.99	2.48	13.80

* Mechanical properties were reported by (Wu et al. 2006b) [21]
** Mechanical properties were reported by (Wu et al. 2006c) [4]
*[a] Mechanical propertied were defined from Table 1.

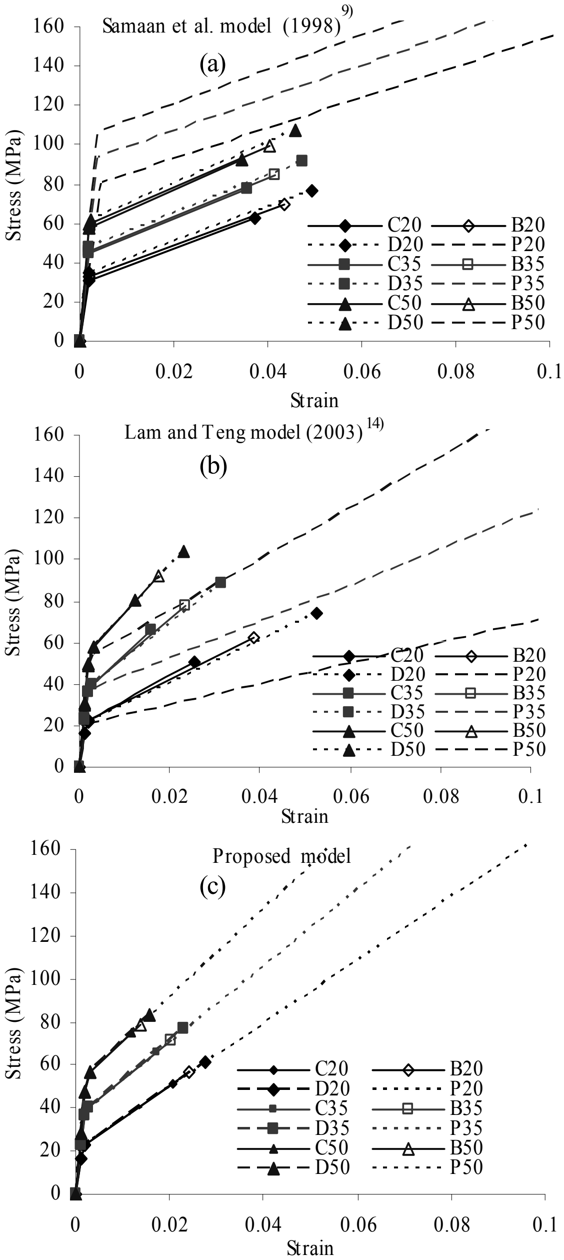

Fig. 2 Predicted axial stress-strain curves of three scale-model circular columns using the model of (a) Samaan et al., (b)Lam and Teng, and (c) this paper

3.2 Accuracy of the Examined Models in Predicting E_2

Prediction of the second stiffness of the stress-strain relationship of FRP-confined concrete is the second measure in this study to evaluate performance of the existing models. A wide-ranging base of experimental data of FRP-wrapped circular specimens is used, and the existing models are directly or indirectly employed to estimate the value of E_2. Samaan et al model proposed direct equations to predict E_2, but Lam and Teng model indirectly calculates E_2 through the given description of the stress-strain curve of confined concrete and the definition of its parameters (f'_{cc}, f_t , and f_o and their corresponding strain values).

(1) Description of Investigated Specimens

In order to compare between these models and examine their accuracy in predicting the second stiffness, test results of 249 FRP-wrapped plain concrete cylinders were collected from the existing literature. The employed fibers were wrapped on concrete cylinders with the main fibers running in the hoop direction, so the resulting FRP jacket had an insignificant stiffness in the axial direction. The database contains 76 specimens assembled by Lam and Teng (2003) [14] from an extensive survey at that time, and 8 specimens from those assembled by Campione and Miraglia (2003) [22]. The other 165 specimens collected by the authors, were reported by Toutanji (1999) [12], Shahawy et al. (2000) [23], Karabinis and Rousakis (2002) [24], Harries and Kharel (2003) [25], Berhet et al. (2005) [26], Mandal et al (2005) [27], Wu et al (2006a) [16], Almusallam (2007) [28], and Youssef et al. (2007) [29]. Some specimens of this database were nominally identical, hence, the average performance (average of two, three, or five experimental results) is considered in this study and finally the entire specimens are 115 in number (72 specimens with $f'_{co} \leq 40$ MPa. and 43 with $f'_{co} > 40$ MPa.). It is noteworthy that all specimens of the database exhibited strain hardening performance. In addition, all specimens in the present database failed by the rupture of the FRP jacket due to hoop tension, and specimens with other failure modes were not included. The prepared database covers a wide range of parameters, which may be summarized below:

- Cylinder size varies from small-test to large-scale specimens. Diameter and height range from 70mm to 407mm and 140mm to 813mm, respectively.
- Concrete compressive strength ranges from 19.4 to 169.7 MPa.
- Different confinement materials are used such as, carbon, glass, and aramid FRP, with a range of thickness from 0.11 to 5.84 mm, and a Young's modulus from 13.6 to 629.6 GPa. The carbon fibers used include high strength and high modulus carbon fibers.
- FRP tensile strengths of some samples were provided by manufacturers, and for other samples were determined by coupon tests.

The distribution of the percentage ratios of the predicted-to-experimental second stiffness according to the different addressed models are shown in **Fig.3**. Statistical results (average ratio (Avg.), standard deviation ratio (SD), and coefficient of variation ratio (COV)) of each model are shown in **Table 4**.

Table 4 Statistical results of the studied models

Source of models	Avg. (%)	SD (%)	COF (%)
Samaan et al. (1998) [9]	65.6	23.0	**35.0**
Lam and Teng (2003) [14]	**100.3**	36.1	36.0
Proposed model	**100.3**	**27.9**	**27.8**

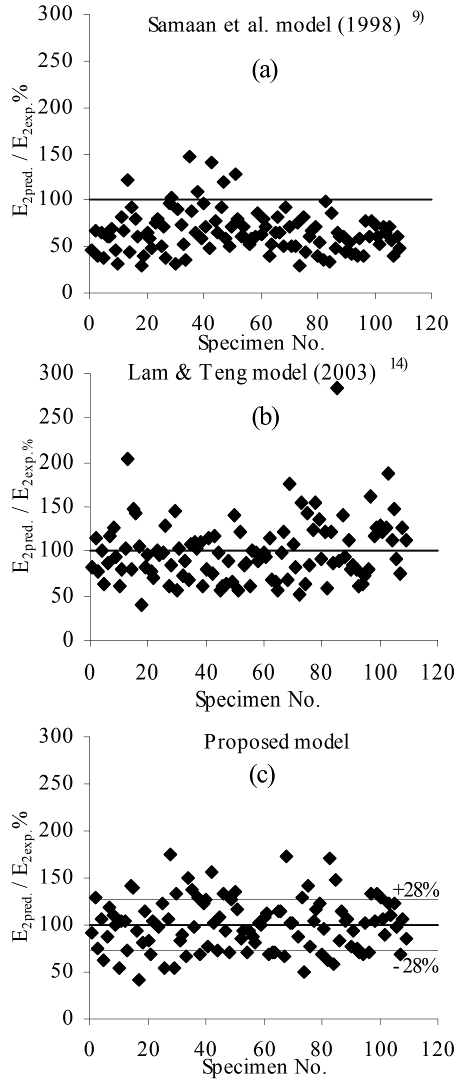

Fig. 3 Predicted-to-experimental ratio of E_2 using the model of (a) Samaan et al, (b) Lam and Teng, and (c) this paper

From **Fig.3(a)** and **Table 4**, it is evident that Samaan et al model, in a comparison with the results of Lam and Teng model, exhibited a lower level of dispersion, with a coefficient of variation of 35.0%. Meanwhile, the average ratio (65.6%) demonstrates that the model is a conservative one. Lam and Teng model, **Fig. 3(b)**, is the least conservative model with average ratio of 100.3%, but the coefficient of variation value (36.0%) reflects some discrepancy between the model predictions and experimental data.

4. Detailed Discussion of Features and Accuracy of both Models

This section presents a more detailed discussion about the validity, accuracy, features, and special issues of Samaan et al. and Lam and Teng models.

4.1 Samaan et al. Model

Samaan et al. (1998) [9] assumed one empirical form to predict the slope of the second branch of the stress-strain relationship. The parameters of this equation are the unconfined concrete strength and the FRP confinement modulus, so, this equation verifies that the slope of the second branch is the same in case of different types of FRP providing equivalent lateral stiffness, **Fig.2(a)**. All the predicted slopes of the second branch in each case of the three columns are parallel, and regarding to the used fiber they have different ultimate strains. However, the predicted curves finally are not coincident, which is an indication that this model still has one drawback or more. The discrepancy of these curves is explicit in the three columns confined with PET (P20, P35, and P50) in a comparison with the others, **Fig.2(a)**. The main reason of this weakness is the definition of the starting point of the second slope. It was suggested by Samaan et al. (1998) [9] that the second slope of the stress-strain curve is intersecting the stress axis at f_o, which is a function of FRP ultimate lateral pressure. This means that upward shifting of the second branch is expected by the increase of the ultimate lateral pressure, which has an indirect relation with the stiffness of the used fiber. Consequently, the maximum upward shifting of the predicted curves of **Fig. 2(a)** is noticed for samples wrapped with PET which has the minimum stiffness and in turn the highest ultimate lateral pressure. In addition, the statistical analysis of this model results for the slope E_2 in view of the available database demonstrated that the model is a conservative one and the predicted results are with somewhat a low level of dispersion. This underestimation may be attributed to the small number of the tested samples (30 cylindrical specimens) that were used to calibrate the constants of the proposed empirical equations of this model.

4.2 Lam and Teng Model

Lam and Teng model is a design-oriented model based on a reliable database of small cylinders confined with the common FRP, and it showed a good accuracy for predicting E_2 in view of the available experimental data, **Fig. 3(b)**. However, dependence of this model on the actual rupture strain of FRP limits its use. It would be difficult to reliably predict the stress-strain relationship of FRP-confined circular columns without additional information about the rupture strain of new types of FRP. It was reported by Lam and Teng (2003) [14] that if this information is not available from the manufacturer, the user should conduct these testes instead. But for design purpose it is not convenient to depend on this supposition while there are many factors that may control the rupture strain of each type of the available FRP composites (concrete strength, sample size, lateral stiffness, etc.).

Lam and Teng model was used to predict the stress-strain responses of the scale-model columns using CFRP, BFRP, DFRP, and PET as confining materials, **Fig.2(b)**. But, the FRP efficiency factors of Basalt, Dyneema, and PET were not given at that paper. To compare these materials in case of equivalent lateral stiffnesses, the efficiency factors was assumed 0.63, which is the average of the efficiency factors of all results of the database by Lam and Teng (2003). Even so, it is clear from **Fig.2(b)** that the predicted slopes of each column are different: the stress-strain curves are incoincident and the second slopes of any concrete strength start from different transition points. This reveals that this model has some drawbacks in its definition to the parameters of the stress-strain curve. First, E_2 is indirectly evaluated via separate equations of the ultimate strength and strain of FRP-confined concrete, which are mainly depending on a variable parameter according to the type of FRP. Second, the definition of the stress and strain at the transition point is a function of E_2, which sequentially is a function of the FRP efficiency factor.

5. Constitutive Stress-Strain Relationship

Throughout the above comparisons, the following problems were identified in applying these models in practice. Both models failed to satisfy the criterion that stress-strain responses of concrete confined with different offered fibers are coincident with different end points in case all types of fibers are designed to the same level of lateral stiffness to select one for confinement. The suggested mathematical forms of these models interpreted their own test results or data used, and are not appropriate for the general practical application. The underestimation of the investigated models to E_2 and the high level of dispersion lead to uneconomic or unsafe application of these models for strengthening structures, particularly, for structures with highly demand of strength and ductility. Based on the above brief discussion, a reliable model for predicting the stress-strain relationship is still lacking. Therefore, a new model will be proposed and discussed in this section.

5.1 Proposed Stress-Strain Model

Simplicity of the described stress-strain response of FRP-confined concrete by Lam and Teng (2003) [14], effectively prodding the authors to take up the same assumptions to describe this relation. Thus, the description of the stress-strain response of FRP-confined is two parts. The first is parabolic smoothly meeting with the second ascending part of the stress-strain relationship, which is linear with a slope E_2 that intersects the stress axis at f'_{co}. Of course, this assumption will eliminate the problem of different starting points of the second ascending part, in case different fibers are elected to decide on one for confinement.

(1) First Ascending Part

To generate the first ascending parabolic part of the stress-strain curve, proposed equations by Lam and Teng (2003) [14] are utilized here, Eqs. (10 to 13). Those equations are function of the elastic modulus E_c of unconfined concrete and the second slope E_2 of the stress-strain relationship of FRP-confined concrete.

(2) Second Stiffness (E_2)

The second slope of the stress-strain response should be directly estimated through one equation. The proposed mathematical form should reflect the effect of both the lateral stiffness of the used fiber and unconfined compressive strength on E_2. By this way, a general circuit definition for the parameters of the stress-strain relationship is guaranteed, wherever the impact of FRP confining material is considered throughout the provided lateral stiffness, which is independent of FRP type.

The proposed equation by Samaan et al (1998) [9] to estimate the slope of the second branch of the stress-strain curve reflects the effect of both unconfined concrete strength and the confinement modulus of FRP composites. But, the results of this equation are conservative with a somewhat high discrepancy, **Fig.3 (a)**. Thus, this equation is adopted here and its constants will be adjusted through a calibration process using the available database. Accordingly, the equation may be re-expressed in a general form as:

$$E_2 = m_2\left(245.61 f_{co}^{'\ m_1} + 0.6728 E_l\right) \tag{18}$$

where m_1 and m_2 are constants that may be determined from the available experimental results. The strategy of calibrating these constants depends on assuming the value of $m_2 = 1$ and increasing the value of m_1 from 0.2, as assumed by Samaan et al (1998) [9], to 0.3, 0.4, etc., till the highest accuracy is met. The highest level of accuracy is indicated by the lowest level of dispersion. This calibration depends on the assumption of increasing the effect of unconfined concrete strength on E_2. The calibration results are summarized in **Fig.4**. It is clear that a good accuracy was when m_1 = 0.43. The average ratio is 100.6% and coefficient of variation is 29.2%.

Since the concrete compressive strength in the current database ranges from 19.4 to 169.7 MPa, this adjustment may be unreliable. It is believed that there is an indirect relationship between the unconfined concrete compressive strength and E_2, i.e., E_2 is highly affected by low strength concrete than high strength concrete. Throughout the calibration process it was noticed that two equations would be a reasonable assumption to consider the effect of concrete strength on E_2. Relationship between the experimental results and the predicted values of E_2 using Eq. (18) is plotted in **Figs.5(a and b)**, when m_2 equals 0.2 and 0.5, respectively. It is clear that two trend lines could rationally predict E_2 with reference to the unconfined concrete strength of 40 MPa.

Tracking the change in the coefficient of variation for both specimens with $f'_{co} \leq 40$ MPa and those with $f'_{co} > 40$ MPa, it was found that its value changed, respectively, from 35.8% to 28.2% and from 27.5% to 30.7%, **Fig. 4**. Therefore, another calibration process is considered. In this process, m_2 was selected to be 0.5 when unconfined concrete strength is less than 40 MPa and 0.2 in case it is over this limit. The values of m_1, guaranteeing the requirement of lowest level of dispersion, were calibrated by the available experimental results. These values are 0.83 and 1.73 corresponding to the values (0.5 and 0.2) of m_2, respectively. The average ratio of the predicted-to-experimental E_2 and the coefficient of variation are 100.2% and 28.4%, respectively, for specimens with $f'_{co} \leq$ 40MPa, and are 100.3% and 27.5%, respectively, for those with $f'_{co} >$ 40MPa, **Fig. 6**.

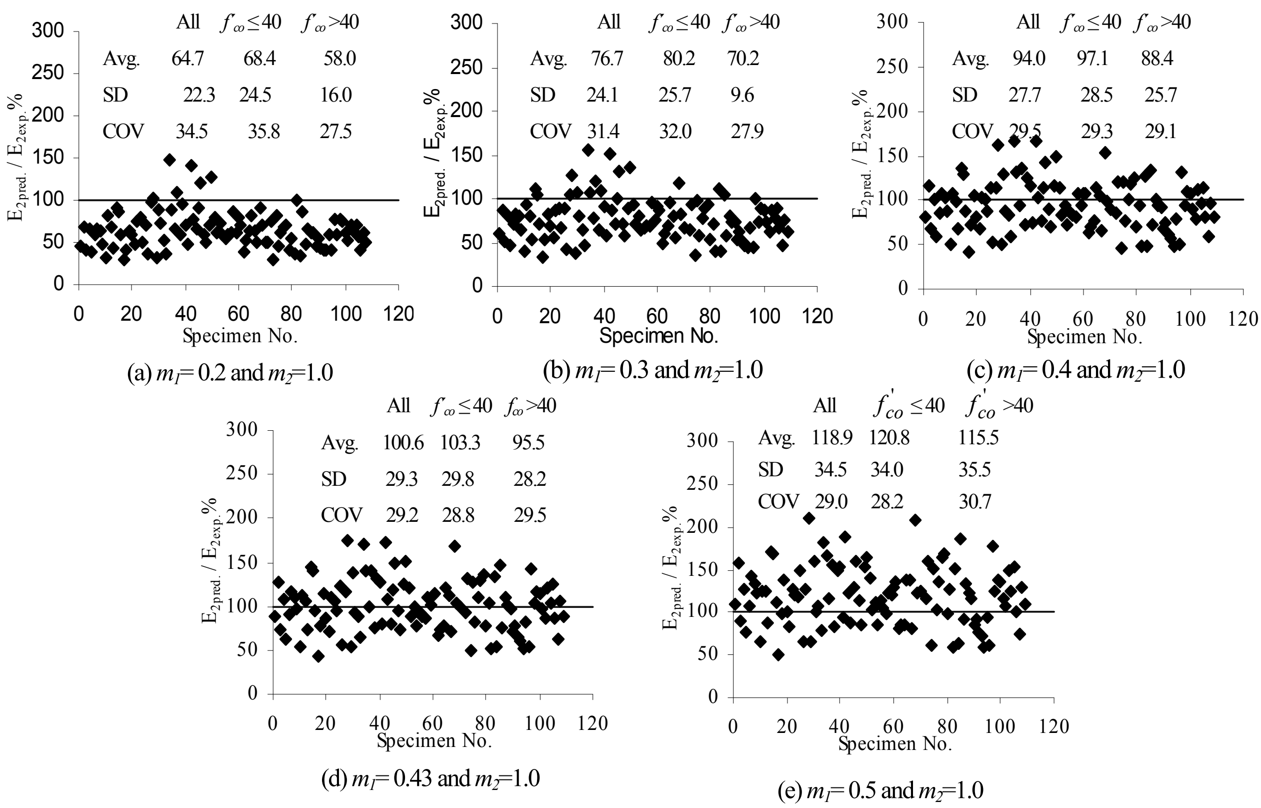

(a) m_1= 0.2 and m_2=1.0 (b) m_1= 0.3 and m_2=1.0 (c) m_1= 0.4 and m_2=1.0

(d) m_1= 0.43 and m_2=1.0 (e) m_1= 0.5 and m_2=1.0

Fig. 4 Calibration process of the constants m_1 and m_2 of the proposed model

Ultimately, the proposed equation to estimate the slope of the second stage of stress-strain response of FRP-confined concrete is expressed as follows:

$$E_2 = m_2\left(245.61 f_{co}^{'\,m_1} + 0.6724 E_l\right) \tag{19}$$

$$m_1 = 0.5,\ \ m_2 = 0.83\ \ f_{co}^{'} \le 40MPa$$
$$m_1 = 0.2,\ \ m_2 = 1.73\ \ f_{co}^{'} > 40MPa$$

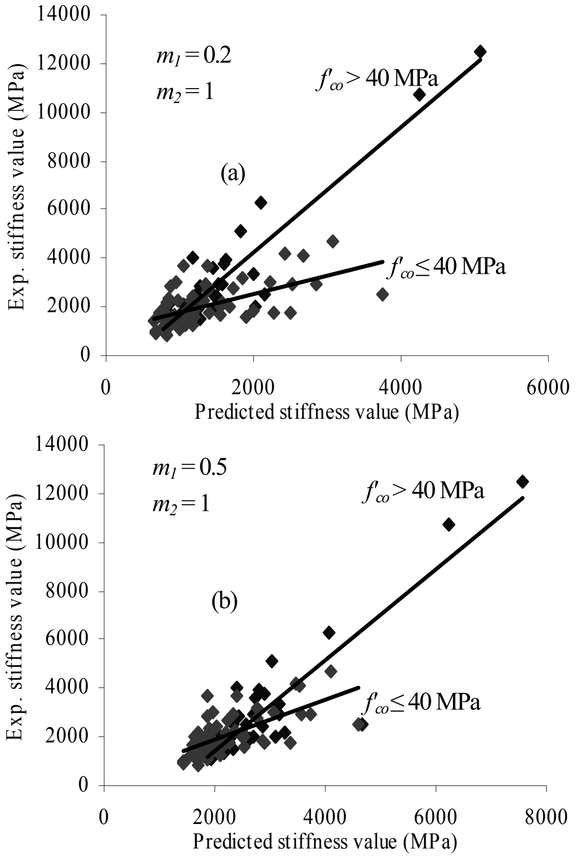

Fig.5 Effect of unconfined concrete strength on evaluation of E_2 in case of m_2 =1 and m_l = (a) 0.2 and (b) 0.5

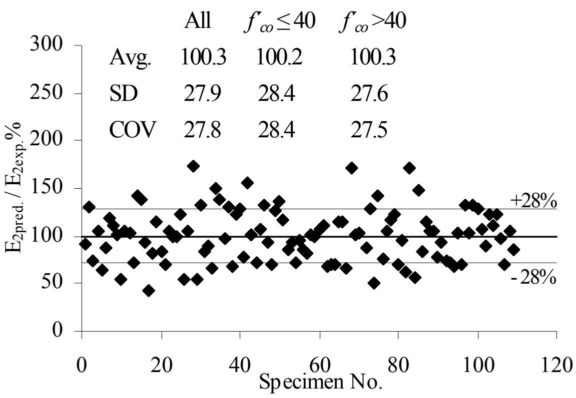

Fig.6 Accuracy of the proposed model to evaluate the slope E_2 of FRP-confined concrete

(3) Endpoint of Stress-Strain Relationship

Here, the ultimate strength will be used to define the end point of the stress-strain relationship, since Bisby et al. (2005) [30] concluded that the discrepancy in the results of the applied forms to estimate the ultimate strength of FRP-confined concrete is less than that to predict the ultimate strain. To find the equation that can predict the ultimate strength with a good accuracy, both of the investigated models were used in view of the available database. Statistical results (average ratio of the predicted-to-experimental ultimate strength, standard deviation ratio, and coefficient of variation ratio) for both models are shown in **Table 5**. The lower dispersion is exhibited by Samaan et al. model, where coefficient of variation is 18.1%. But, the average ratio of predicted-to-experimental ultimate strength is 119.3%, that is, the model is overestimating the ultimate strength. To avoid this, K_l of Eq. (5) was calibrated in the light of the available database with explicit consideration to the effect of unconfined concrete compressive strength, **Fig.7**.

$$k_1 = 3.5 f_{lu}^{-0.3} \qquad f'_{co} \le 40\text{MPa}, \tag{20}$$

$$k_1 = 4.5 f_{lu}^{-0.3} \qquad f'_{co} > 40\text{MPa}, \tag{21}$$

Table 5 Statistical results of the studied models to predict the ultimate strength

Source of models	Avg. (%)	SD (%)	COV (%)
Samaan et al. (1998) [9]	119.3	21.6	**18.1**
Lam and Teng (2003) [14]	107.5	23.5	21.9
Proposed model	**100.1**	**16.6**	**16.6**

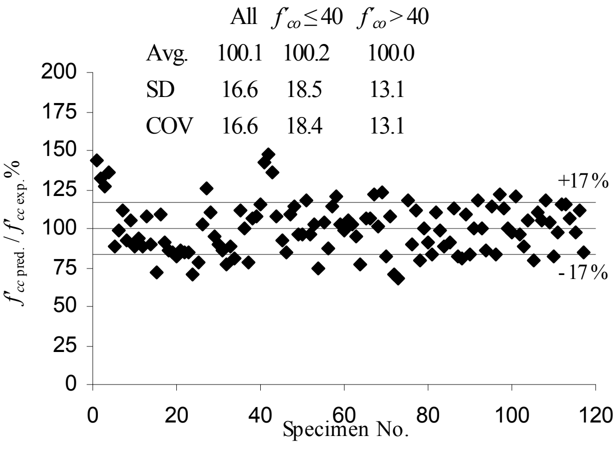

Fig.7 Accuracy of the proposed model to evaluate the ultimate strength of FRP-confined concrete

5.2 Accuracy Verification of the Proposed Model

The proposed stress-strain model of FRP-confined concrete is compared with the test data on FRP-wrapped concrete cylinders by Shahawy et al. (2000) [23], Berhet et al. (2005) [26], and Youssef et al. (2007) [29]. The variables considered in this verification are concrete strength, specimen size, FRP composites (CFRP and GFRP), confinement modulus (number of layers), and sources defined the ultimate tensile strength of FRP materials (coupon tests or manufacturers). The details of these samples are summarized herein. Cylinders with unconfined concrete compressive strength 19.4 and 49 MPa were tested by Shahawy et al. (2000) [23]. The size of those cylinders was 152.5 mm diameter by 305 mm height. Thickness of one layer of the used CFRP was 0.5 mm with ultimate tensile strength and elastic modulus 2275 MPa and 82.7 GPa, respectively, determined by the original authors. A wide range of unconfined concrete compressive strength was tested by Berhet et al. (2005) [26] starting from 25 MPa to 169.7 MPa. For high strength concrete (f'_{co} = 112.6 and 169.7 MPa), the size of the tested specimen was 70 mm diameter and 140mm height, but other specimens size was 160mm diameter and 320 mm height. CFRP and GFRP were used for confinement, and their mechanical properties were given by manufactures as (t = 0.165 mm, f_{ju} = 3200 MPa, and E_j = 230 GPa) and (t = 0.165 mm, f_{ju} = 2500 MPa, and E_j = 75 GPa), respectively.

The accuracy of the proposed model for predicting the stress-strain response of large scale samples was verified by comparing the model results with the test results of Youssef et al. (2007). The results by Youssef et al. (2007) [29] are the average of three tested nominally identical samples with unconfined compressive strength ≈ 40 MPa. The dimensions of the tested samples were 406 mm diameter and 813 mm height. CFRP was used as a confinement material, and its mechanical properties, provided by manufactures, are (t = 0.584 mm, f_{ju} = 1246 MPa, and E_j = 103.8 GPa). In an attempt to verify further the accuracy of the proposed model, these test results were compared with the analytical predictions of Lam and Teng model. Also, the proposed model is applied to predict the stress-strain responses of FRP-confined concrete of the scale-model columns, considering the offered FRPs and the design condition of equivalent lateral modulus.

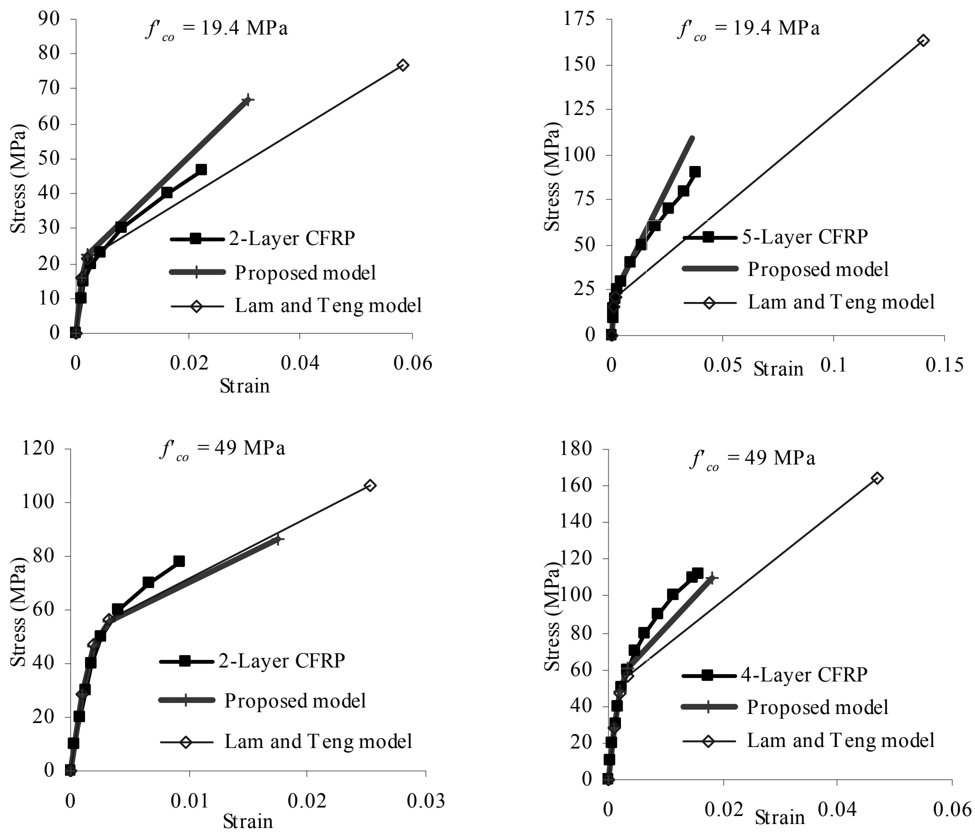

Fig.8 Comparison between test results of Shahawy et al. (2000) [23] and the predicted stress-strain curves using the proposed model and Lam and Teng model

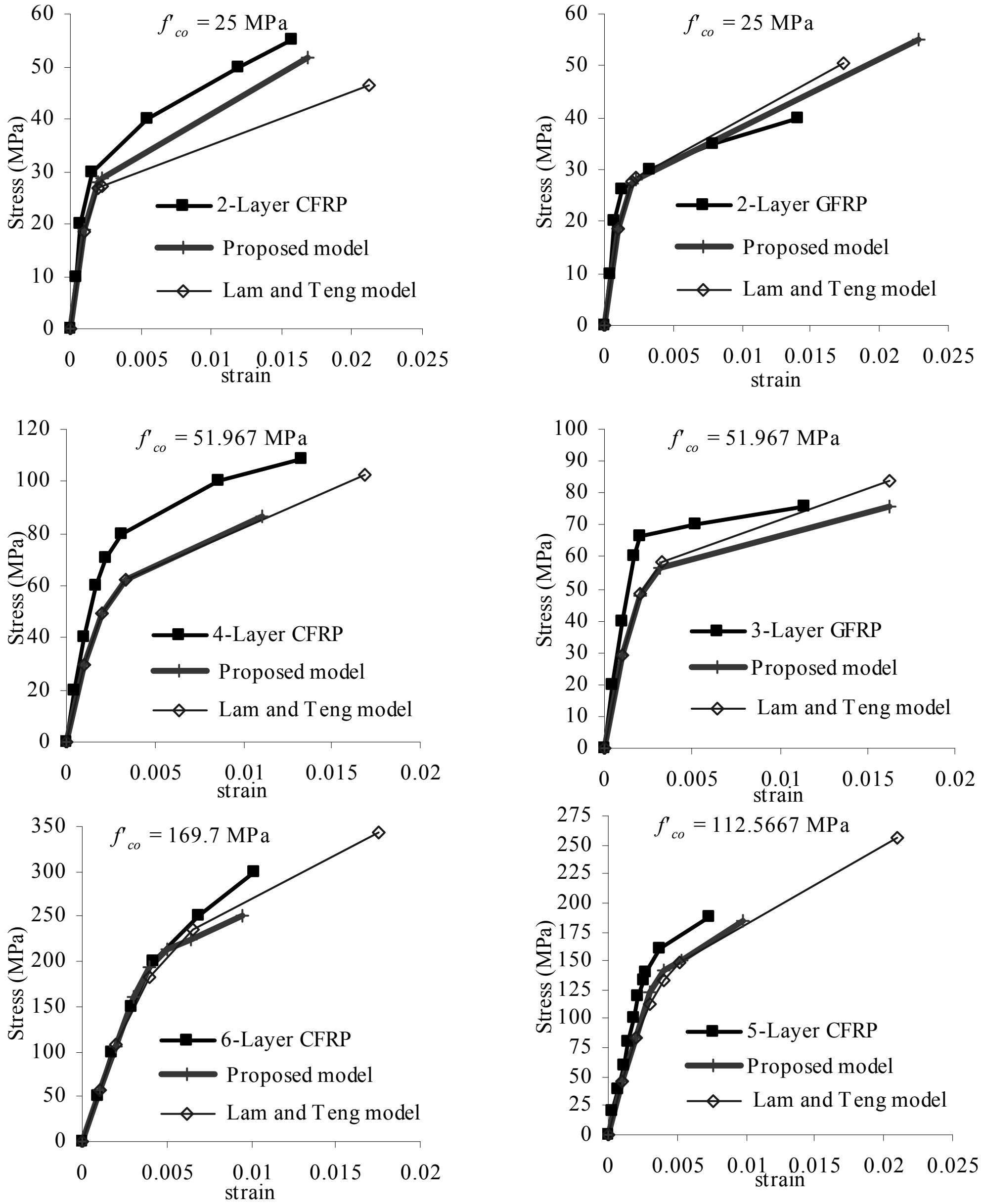

Fig.9 Comparison between test results of Berhet et al. (2005) [26] and the predicted stress-strain curves using the proposed model and Lam and Teng model

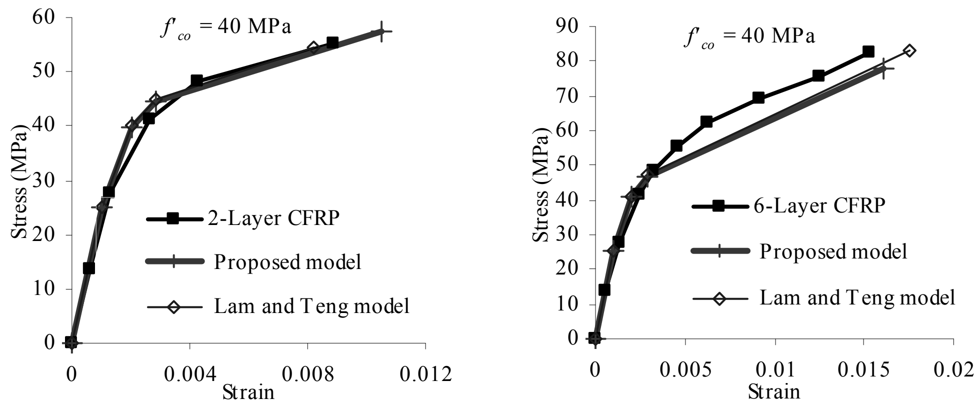

Fig.10 Comparison between test results of Youssef et al. (2007) [29] and the predicted stress-strain curves using the proposed model and Lam and Teng model

It is clear from **Figs.8-10** that the proposed model predicts the stress-strain response of FRP-confined concrete, having a wide range of parameters, with a reasonable accuracy. The predicted stress-strain responses of any of the scale-model columns, **Fig.2(c)**, are entirely coincident with different endpoints: the proposed model could be used as a general model for FRP-confined circular columns.

In future studies, the more the available database covering other parameters and including samples confined with the new types of FRP, the higher the accuracy of the proposed model.

6. Conclusions

This paper carried out a comparison between two models (Samaan et al. (1998) [9] model and Lam and Teng (2003) [14] model) in order to check their validity and accuracy for general application. Test results of 249 cylinder specimens collected from the existing literature were used in the current comparison. According to the criteria of each model, the stress-strain responses of FRP-confined concrete of three scale-model columns with different unconfined concrete compressive strengths (20, 35, and 50 MPa) were predicted, provided the lateral stiffness of the offered FRPs are the same. Also, these models have been evaluated through the prediction of the slope of the second branch of the stress-strain curves of the available experimental results. Finally, Samaan et al. model has been adopted and a new model has been proposed based on a statistical analysis. Furthermore, the proposed stress-strain model for FRP-confined concrete has been verified through a comparison with the test data of FRP-wrapped concrete cylinders by Shahawy et al. (2000) [23], Berhet et al. (2005) [26], and Youssef et al. (2007) [29]. Based on the results of the current study, the following conclusions may be drawn: (1) The examined models failed to satisfy the criterion that stress-strain responses of concrete confined with different offered fibers are coincident with different end points in case all types of fibers are designed to the same level of lateral stiffness. (2) While Lam and Teng model indirectly estimates the slope of the second branch of the stress-strain relationship of confined concrete, the model showed a good accuracy for predicting E_2. However, the model is not suitable for the general practical application due to its dependence on the actual rupture strain of FRP to predict the ultimate strength and strain of confined concrete. (3) The performance of the proposed model in this paper can improve the inadequacies of the pre-investigated models, where definitions of the parameters of the stress-strain relationship are interrelated and reflect the impact of FRP confining material throughout the provided lateral stiffness, rather than the ultimate lateral pressure, which is only considered responsible for the definition of the endpoint of this relationship. (4) Since the proposed model has been calibrated against a relatively large database than that used by the other investigated models, and it covers a wide range of different parameters; it is believed that the proposed model can give a realistic prediction of the stress-strain response of FRP-confined concrete, in addition to its simplicity in application.

REFERENCES

1) Japan Society of Civil Engineering (JSCE), Applications of innovative composite material for civil engineering, *Research Committee Report*, 2005.
2) Wu, Z. S., Iwashita, K., Hayashi, K., Higuchi, T., Murakami, S., and Koseki, Y., Strengthening prestressed-concrete girders with externally prestressed PBO fiber reinforced polymer sheets, *J. Reinf. Plas. Compos*. 22(14), pp.1269-1286, 2003b.
3) Wu, Z. S., Wang, X., and Iwashita, K., State-of-the-Art of advanced FRP applications in civil infrastructure in Japan, *CD-ROM of Compos. & Polycon*, *American Composites Manufacturers Association,* Tampa, FL USA**.** 2007b.
4) Wu, Z. S., Gu, D. S., Wu, G., and Hirahata, H., Seismic performance of RC columns strengthened with dyneema fiber-reinforced polymer sheets, *Proc., 4th Inter. Confe. of Earthquake Enger. (ICEE2006)*, Taipei, Taiwan. Paper No. 157, 2006c.
5) Anggawidjaja, D., Ueda, T., Dai, J., and Nakai, H., Deformation capacity of RC piers by new fiber-reinforced polymer with large fracture strain, *Cem. & Conc. Compos.* 28, pp.914-927, 2006.
6) Wu, G., Gu, D. S., Wu, Z. S., Jiang, J. B., and Hu, X. Q., Comparative study on seismic performance of circular concrete columns strengthened with BFRP and CFRP composites, *Poce., Asia-Pacific Conference on FRP in Structures (APFIS 2007)*, Hong Kong, China.Vol.1, pp.199-204, 2007a.
7) Fardis, M. N., and Khalili, H., FRP-encased concrete as a structural material, *Mag. Conc. Res.* 34(121), pp.191-202, 1982.
8) Karbhari, V. M. and Gao, Y., Composite jacketed concrete under uniaxial compression-Verification of simple design equations, *J. Mater. Civil Eng.*, ASCE. 9(4), pp.185-193, 1997.
9) Samaan, M., Mirmiran, A., and Shahawy, M., Model of concrete confined by fiber composites, *J. Struct. Enger.*, ASCE. 124(9), pp.1025-1031, 1998.
10) Saafi, M., Toutanji, H. A., and Li, Z., Behavior of concrete columns confined with fiber reinforced polymer tubes, *ACI Mater. J.* 96(4), pp.500-509, 1999.
11) Hosotani, M. and Kawashima, K., A stress-strain model for concrete cylinders confined by both carbon fiber sheets and tie reinforcement, *J. Conc. Enger.*, JSCE. 620/43, pp.25-42, 1999.
12) Toutanji, H.A., Stress-strain characteristics of concrete columns externally confined with advanced fiber composite sheets, *ACI Mater. J.* 96(3), pp.397-404, 1999.
13) Xiao, Y. and Wu, H., Compressive behavior of concrete confined by carbon fiber composite jackets, *J. Mater. Civ. Enger.* ASCE. 12(2), pp.139-146, 2000.
14) Lam, L. and Teng, J. G., Design-oriented stress-strain model for FRP-confined concrete, *Constr. Buil. Mater.* 17, pp.471-489, 2003.
15) Wu, G., Lu, Z. T., and Wu, Z. S., Stress-strain relationship for FRP-confined concrete cylinders, *Proc., 6th Intern. Sympo. on FRP Reinfor. for Conc. Struct. (FRPRCS)*, Singapore,

pp.552-560, 2003a.

16) Wu, G., Lu, Z. T., and Wu, Z. S., Strength and ductility of concrete cylinders confined with FRP composites, *J. Constr. Buil. Mater.* 20, pp.134-148, 2006a.

17) Harajli, M. H., Axial stress-strain relationship for FRP confined circular and rectangular concrete columns, *Cement &Conc. Compos*. 28, pp.938-948, 2006.

18) Chang, S.-Y., Li, Y.-F., and Loh, C. H, Experimental study of seismic behaviors of as-built and carbon fiber reinforced plastics repaired reinforced concrete bridge columns, *J. Br. Enger.*, ASCE. 9(4), pp.391-402, 2004.

19) Richart, F. E., Brandtzaeg, A., and Brown, R. L., A study of the failure of concrete under combined compressive stresses, *Bulletin 185,* University of Illinois Engineering Experimental Station, Champaign, I11, 1928.

20) De Lorenzis, L. and Tepfers, R., Comparative study of models on confinement of concrete cylinders with fiber-reinforced polymer composites, *J. Compos. Constr.*, ASCE. 7(3), pp.219-237, 2003.

21) Wu, G., Wu, Z. S., Lu, Z. T., and Gu, D. S., Seismic retrofit of large scale circular columns wrapped with CFRP sheets, *Proc., 3rd Inter. Confe. of FRP Compos. In Civil Engrg. (CICE2006)*, Miami, Florida, USA. pp.547-550, 2006b.

22) Campione, G. and Miraglia, N., Strength and strain capacities of concrete compression members reinforced with FRP, *Cem. & Conc. Compos.* 25, pp.31-41, 2003.

23) Shahawy, M., Mirmiran, A., and Beitelman, T., Tests and modeling of carbon-wrapped concrete columns, *Compos.: Part B.* 31, pp.471—480, 2000.

24) Karabinis, A. I. and Rousakis, T. C., Concrete confined by FRP material: a plasticity approach, *Enger. Struct.* 24, pp.923-932, 2002.

25) Harries, K. A. and Kharel, G., Experimental investigation of the behavior of variably confined concrete, *Cem. & Conc. Research.* 33, pp. 873-880, 2003.

26) Berhet, J. F., Ferrier, E., and Hamelin, P., Compressive behavior of concrete externally confined by composite jackets. Part A: experimental study, *Constr. & Buil. Mater.* 19, pp.223-232, 2005.

27) Mandal, S., Hoskin, A., and Fam, A., Influence of concrete strength on confinement effectiveness of fiber-reinforced polymer circular jackets, *ACI Struct. J.* 102(3), pp.383-392, 2005.

28) Almusallam, T. H., Behavior of normal and high-strength concrete cylinders confined with E-glass/epoxy composite laminates, *Compos.: Part B*. 38, pp.629-639, 2007.

29) Youssef, M. N., Feng, M. Q., and Mosallam, A. S., Stress-strain model for concrete confined by FRP composites, *Compos.: Part B.* 38, pp.614-628, 2007.

30) Bisby, L. A., Dent, A. J. S., and Green, M. F., Comparison of confinement models for fiber-reinforced polymer-wrapped concrete, ACI *Struct. J.* 102(1), pp.62-72, 2005.

(Received: April 9, 2009)